



# Contribution of standardized indexes to understand groundwater level fluctuations in response to meteorological conditions in cold and humid climates

Emmanuel Dubois<sup>a,b,\*</sup>, Marie Larocque<sup>b,c</sup>

<sup>a</sup> Platform of Hydraulic Constructions (PL-LCH), IIC, School of Architecture, Civil and Environmental Engineering (ENAC), Ecole Polytechnique Fédérale de Lausanne (EPFL), Lausanne, Switzerland

<sup>b</sup> Université du Québec à Montréal (UQAM), Département des sciences de la Terre et de l'atmosphère, GEOTOP Research Center, Montréal, Canada

<sup>c</sup> GRIL Research Center, Département de sciences biologiques, Université de Montréal, Montréal, Canada

## ARTICLE INFO

This manuscript was handled by Corrado Corradini, Editor-in-Chief

### Keywords:

Groundwater level  
Precipitation  
Temperature  
Global climate indexes  
Standardized indexes  
Cold and humid climates  
Drought

## ABSTRACT

Understanding the fluctuations in groundwater levels in response to meteorological conditions is challenging, especially given the slow transit time associated with groundwater reservoirs and the short duration of time series for groundwater levels. Nevertheless, this knowledge is crucial for water resource management, especially given that global warming will drastically impact the hydrological dynamics in cold and humid climates. The objective of this work was to quantify how standardized indexes contribute to understanding groundwater level fluctuations in response to meteorological conditions in cold and humid climates and with short time series (10 to 23 years). The relationships between the standardized precipitation index (SPI), standardized temperature index (STI), global climate indexes, and standardized groundwater index (SGI) were analyzed. The reactivity of groundwater levels was examined between 2000 and 2022 using groundwater level measurements from 152 wells located between 46 °N and 52 °N in the province of Quebec (Canada). The results showed that the available time series were sufficient to provide new insights into the role of precipitation and temperature on groundwater fluctuations, demonstrating the usefulness of the indexes. One of the main contributions of this study was that hydrogeological systems in cold and humid climates go through an annual reset due to the prolonged freezing period. This annual reset was one of the drivers isolating year-to-year hydrogeological conditions, contributing to short-duration droughts.

## 1. Introduction

Increased water use and climate change cause substantial alterations in surface water and groundwater availability throughout the world (de Graaf et al., 2019; Konapala et al., 2020; Scanlon et al., 2023; Van Loon et al., 2022). Hydrological droughts, when groundwater levels remain below a certain level for a long period causing low flow rates and low lake levels (Van Loon, 2015), caused by these changes can have a dramatic impact on populations, ecosystems, agriculture, and industries (Krogulec, 2018). With slower transit times, groundwater reservoirs tend to buffer the more active surface flow processes, increasing the resilience of water resources but delaying the response to changing conditions at the surface (Cuthbert et al., 2023; Hellwig et al., 2020; de Graaf et al., 2019). Understanding groundwater level fluctuations in

response to meteorological conditions poses specific challenges, most notably because groundwater monitoring networks often cover relatively short time periods and vary in quality (Condon et al., 2021). Identifying groundwater level reactivity and trends in cold and humid climates also brings challenges related to the complex processes associated with soil frost, snow accumulation, snow melt, and spring rain conditions (Aygün et al., 2020). A deeper understanding of reactivity and trends is crucial to better manage groundwater.

Groundwater monitoring wells provide observational windows into aquifers for specific locations where the groundwater level is influenced by geology, slope, land use, position in the watershed, proximity to the hydrographic network, climatic conditions, and groundwater pumping (Giese et al., 2020). Groundwater measurements that are collected over longer durations lead to improved monitoring quality and usefulness. In

\* Corresponding author at: Platform of Hydraulic Constructions (PL-LCH), IIC, School of Architecture, Civil and Environmental Engineering (ENAC), Ecole Polytechnique Fédérale de Lausanne (EPFL), Lausanne, Switzerland.

E-mail address: [emmanuel.dubois@epfl.ch](mailto:emmanuel.dubois@epfl.ch) (E. Dubois).

<https://doi.org/10.1016/j.jhydrol.2024.131105>

Received 12 October 2023; Received in revised form 6 March 2024; Accepted 8 March 2024

Available online 24 March 2024

0022-1694/© 2024 The Author(s). Published by Elsevier B.V. This is an open access article under the CC BY license (<http://creativecommons.org/licenses/by/4.0/>).

some countries, these groundwater time series have been available for many years and provide a unique understanding of how groundwater resources vary through time (Marchant and Bloomfield, 2018) and how they are connected to other components of the water cycle (Kuss and Gurdak, 2014; Nygren et al., 2020). In other countries, groundwater level monitoring has started only recently due to insufficient funding or simply because of a relatively new awareness of the possible future scarcity of water resources in a changing climate. For example, in Canada, groundwater level monitoring started in the 1960s (Rivard et al., 2009). However, Canada-wide coverage has only been available since early 2000, when the province of Quebec initiated its own groundwater monitoring network.

Historical trends in groundwater levels represent crucial information for water managers and are increasingly studied throughout the world. The scientific literature reports a mix of increasing and decreasing trends in groundwater levels. Rivard et al. (2009) examined Canada except for the province of Quebec; Guo et al. (2021) examined Georgia, Massachusetts, Oklahoma, and Washington; Jackson et al. (2015) studied the UK; and Nygren et al. (2021) reported on Finland and Sweden. Predominantly decreasing groundwater levels were observed in semi-arid areas of Chile (Valois et al., 2020) while increasing groundwater levels were observed in New England (Dudley and Hodgkins, 2013) and in other US glacial aquifer systems (Hodgkins et al., 2017). The differences in observations were due to varying geological environments, climatic conditions, and the time periods used for analysis. Studies on groundwater droughts have been conducted in several countries (Babre et al., 2022 – Baltic States; Guo et al., 2021 – USA.; Krogulec, 2018 – Poland; Peters et al., 2006 – UK; Secci et al., 2021 – Italy).

Standardized indexes of water cycle variables (e.g., precipitation, temperature, evaporation, flowrates) are increasingly used for these types of studies (e.g., Bloomfield and Marchant, 2013). It is not clear what the advantages and limitations of these indexes are for situations where water scarcity is not an acute problem and when time series data do not span multiple decades. For example, low groundwater level conditions have been recorded in recent years in Quebec (MELCCFP, 2022), pointing to possible future water scarcity. However, the actual extent of these conditions and their underlying causes are not yet understood. These unknowns hinder adaptations in groundwater management policies.

Past studies have identified geological and morphological conditions that either increased or attenuated hydrological droughts. For example, Haslinger et al. (2014) reported that meteorological drought significantly influences streamflow drought, except where groundwater reservoirs and snowmelt processes play an important role in the water cycle. Guo et al. (2021) showed that the response time between meteorological conditions and groundwater drought depends on multiple conditions including location, groundwater pumping for irrigation, and human use. Local, regional, and large-scale meteorological conditions influence groundwater levels, and the link between climate indexes and hydrological conditions is increasingly being studied worldwide (Kuss and Gurdak, 2014).

The complexity of these interactions makes it difficult to identify causal links when there are no clear trends. Adding to this complexity and the limitations inherent to short time series, multi-year climate variability influences the water cycle in a cyclic manner. For example, in eastern Canada, the North Atlantic Oscillation (NAO), the Atlantic Multi-decadal Oscillation (AMO), and the Pacific Decadal Oscillation (PDO) climate indexes influence winter precipitation and temperature, as well as the timing, duration, and extent of flood frequencies (Assani et al., 2019; Assani and Guerfi, 2017; Beauchamp et al., 2015; Mazouz et al., 2013). Tremblay et al. (2011) have also shown that the NAO, the Arctic oscillation (AO), and the Pacific/ North American teleconnection pattern (PNA) partly explain the varying groundwater levels observed in different regions across Canada. However, because long datasets are necessary to assess historical trends, meteorological droughts, and

groundwater droughts, it is not clear whether relatively short time series of groundwater levels can yield useful information when used with climate indexes with different return periods.

The objective of this work was to quantify how standardized indexes contribute to understanding the groundwater level fluctuations observed in response to meteorological conditions in cold and humid climates. These climates are characterized by hydrological dynamics that include a multi-month snow accumulation period and subsequent snowmelt. This research uses data from the province of Quebec (Canada) as a case study, with the expectation that results would be applicable to other cold and humid climates where drought is not yet a recurrent problem. The methods include trend analyses of meteorological variable (precipitation and temperature) time series and a large database of groundwater levels, analyses of standardized indexes for the 2000–2022 period, and identification of causal relationships to explain fluctuations.

## 2. Study area

### 2.1. General context

The study area is located in the southern portion of the province of Quebec (Canada) and covers an area of 980 000 km<sup>2</sup>. The Canada–USA border and the Quebec–New Brunswick border represent the southern limit of the study area. The Grenville geological Province and the Quebec–Labrador border (approximately 52 °N) are the northern limit, the Quebec–Ontario border is the western limit, and the Gulf of St. Lawrence is the eastern limit (Fig. 1). The study area corresponds to the traditional territories of 10 Indigenous Nations, including the Abenaki, Algonquin, Atikamekw, Cree, Innu, Maliseet, Mi'kmaq, Naskapi, Huron-Wendat, and Mohawk. The climate in this area ranges from humid continental in the south to subarctic in the north. Elevations are close to sea level along the St. Lawrence River, up to 950 m above sea level (masl) in the northern portion of the study area and reach 1 200 masl in the southern portion.

### 2.2. Geology and hydrogeology

The study area includes three geological provinces, the metasedimentary Appalachian Province, the sedimentary basin of the St. Lawrence Platform, and the metamorphic Grenville Province (hereafter named the Canadian Shield, its overlying region) (SIGEOM, 2023; Fig. 1). On the south shore of the St. Lawrence River, Quaternary sediments that originate from the previous glaciation–deglaciation cycle primarily consist of thin, coarse material and are found in higher elevation areas. The valleys are characterized by thick, mixed-sized grain deposits. Additionally, large areas of clay deposits (up to tens of meters) inherited from the Champlain Sea overlay the fractured bedrock and sometimes the sandy materials on lower portions of the St. Lawrence Platform. On the north shore, Quaternary sediments of sand and gravel associated with glaciofluvial dynamics are predominantly located in the valleys of the Canadian Shield.

On the south shore, the fractured bedrock aquifer flows regionally from the Appalachians to the St. Lawrence River, in a south-southeast to north-northwest direction (Rivera, 2014). This aquifer is moderately productive and is semi-confined or unconfined above an elevation of approximately 180 masl. In river valleys and in the St. Lawrence Platform, the bedrock aquifer transitions to semi-confined and confined conditions. On the north shore, the fractured bedrock aquifer flows towards the highly productive river valley aquifers and shows limited north-to-south groundwater flow. The aquifer exhibits low productivity but has more productive areas near the fault zones (Rivera, 2014). Both bedrock and valley aquifers may be locally confined beneath thin-grained Quaternary deposits below an elevation of approximately 240 masl.

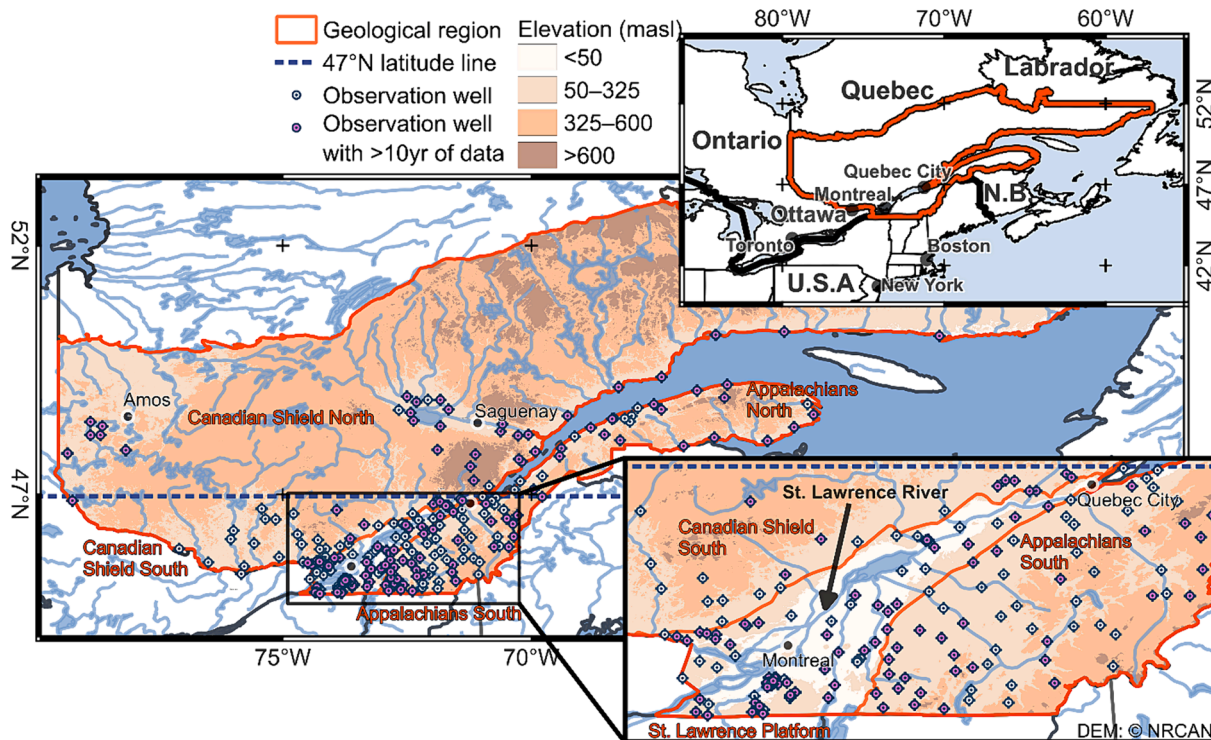


Fig. 1. Location of the study area including geological regions, topography, and observation wells.

2.3. Meteorological conditions

The 2000–2022 interannual average precipitation (sum of liquid and solid precipitation) ranged between 675 mm/yr and 1 400 mm/yr, with the wettest regions (> 1 250 mm/yr) located north of Quebec City and between Sherbrooke and Quebec City. The driest regions (<850 mm/yr) were located mainly north of 51 °N (Fig. 2a). The interannual average temperature ranged between –3 °C and 8 °C, with the warmest regions (> 4 °C) located in the south-western portion of the study area (St. Lawrence Platform) and the coldest area (< 0 °C) located north of approximately 50 °N (Fig. 2b). In the warmest regions (southern study area), rainfall generally occurs until November when temperature drops below 0 °C, followed by precipitation as snowfall until April of the following year when air temperature exceeds again 0 °C. In the coldest regions (northern study area), rainfall generally occurs until October followed by snowfall until April. Snowfall represents 25 % of the annual precipitation in the southernmost parts of the study area and increases until close to 50 % of the annual precipitation in the northernmost parts of the study area.

The three geological units were further subdivided using the 47 °N line as a subjective and approximative line dividing the warmer, southern Quebec (temperature > 4 °C) and the colder, northern Quebec (average temperature < 4 °C) (Fig. 2b). The resulting geological regions and sub-regions are the Appalachians North, the Appalachians South, the St. Lawrence Platform, the Canadian Shield North, and the Canadian Shield South (Fig. 1).

3. Material and methods

3.1. Available data

3.1.1. Groundwater level observation network

In the province of Quebec, wells from the Quebec Groundwater Monitoring Network (*Réseau de suivi des eaux souterraines du Québec*; MELCCFP, 2023a) have been recording hydraulic heads since July 2000. As of December 2022, there were 238 active wells in the study area

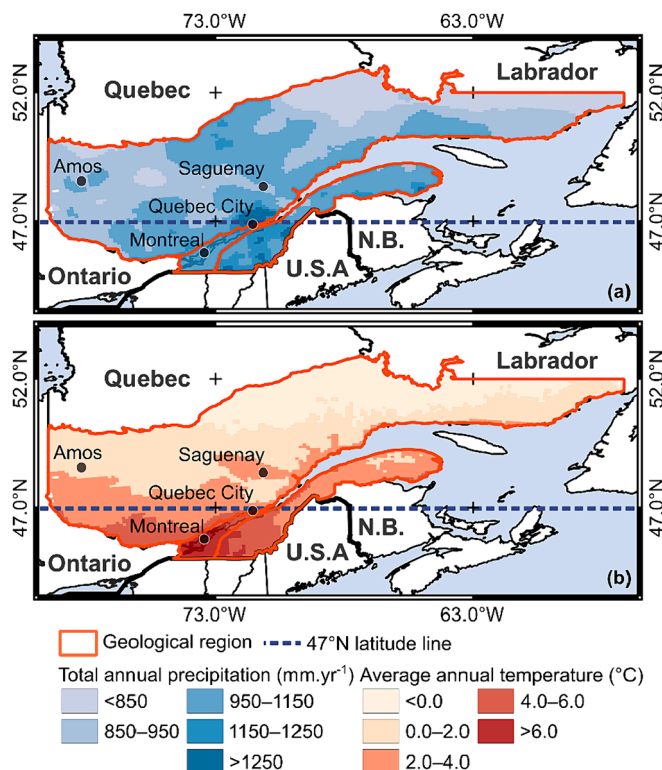


Fig. 2. (a) Average annual precipitation and (b) average annual temperature for the 2000–2022 period (meteorological data from MELCCFP, 2023b).

(Fig. 1). However, only wells with more than 10 years in length and with a maximum of one period of missing data longer than 10 days were used in the analyses. The resulting dataset included 152 wells. The 10-year duration criteria retained the maximum number of wells with the

longest possible time series. The database includes 18 wells located in the Appalachians North, 33 in the Appalachians South, 58 in the St. Lawrence Platform, 33 in the Canadian Shield North, and 10 in the Canadian Shield South (Fig. 3). The wells are located in unconsolidated Quaternary sediments (84 wells) and in the fractured bedrock of the Appalachians or the Canadian Shield (68 wells) in confined (67 wells), semi-confined (21 wells), and unconfined (64 wells) conditions. In the Appalachians South and the St. Lawrence Platform, most observation wells monitored bedrock aquifers (55 % and 64 %, respectively) while in the other regions, most observation wells monitored unconsolidated aquifers (78 % in the Appalachians North, 76 % in the Canadian Shield North, and 90 % in the Canadian Shield South). The average interannual hydraulic head for individual wells varied between 4 masl close to the Gulf of St. Lawrence in the Appalachians North and > 850 masl in the Canadian Shield North, with most hydraulic head values ranging from 50 masl to 250 masl.

### 3.1.2. Gridded climate data and global climate indexes

Interpolated daily precipitation and temperature data at a spatial resolution of 10 km x 10 km were obtained from MELCCFP (2023b; Fig. 2). Based on 375 climate stations located below 52 °N, the root mean square error over the 1961–2017 period was 3 mm/d for daily precipitation and 2.5 °C and 1.5 °C for minimum and maximum daily temperatures, respectively (Bergeron, 2016).

Monthly indexes of the Arctic oscillation (AO; NOAA, 2023a), the North Atlantic oscillation (NAO; NOAA, 2023a), and the Niño 3.4 index (NINO3.4; NOAA, 2023b) were used (Fig. 4). Several studies identified these indexes as the drivers of the interannual variability observed in meteorological conditions and river flow discharge in the province of Quebec (Assani et al., 2022; Assani and Guerfi, 2017; Beauchamp et al., 2015; Mazouz et al., 2013; Qian et al., 2008), and as drivers of groundwater levels in different regions across Canada (Tremblay et al., 2011). These indexes were all characterized by relatively short return periods (AO < 1 yr; NAO ~ 3–6 yr, NINO3.4 ~ 2–7 yr), making them particularly applicable for short time series.

### 3.2. Data treatment

When sub-daily hydraulic head data were available, average daily values were used. The daily values were gap-filled using linear interpolation when ≤ 10 consecutive days had missing values. A running median of seven days was applied to the gap-filled data to smooth out short-term fluctuations. Outliers were identified by examining the differences between the time series and the associated 1-day shifted

version. For a given time series, data points that fell outside the mean difference plus or minus one standard deviation were considered outliers and were therefore removed and replaced by linear interpolation. These data treatment steps ensured the integrity and quality of the groundwater level time series, facilitating subsequent analyses and interpretation of hydrological patterns and anomalies.

Trends in daily precipitation, temperature, and groundwater level data were assessed using the Mann-Kendall test (*kendall* R package) and were considered significant when p-value ≤ 0.05. The magnitude of significant trends was determined using Sen's slope (*kendall* R package). Trends in temperature and precipitation data were calculated for each grid cell while trends in groundwater level data were calculated for each observation well.

### 3.3. Standardized indexes

To compare the changes in groundwater levels with those of precipitation and temperature, time series were modified using the standardized precipitation index (SPI; McKee et al., 1993), the standardized temperature index (STI; Zscheischler et al., 2014), and the standardized groundwater index (SGI; Bloomfield and Marchant, 2013). These indexes have been extensively used to correlate meteorological droughts to hydrological groundwater conditions (Bloomfield and Marchant, 2013; Guo et al., 2021; Kumar et al., 2016; Secci et al., 2021). SPI and STI indexes were calculated by fitting a probabilistic distribution to monthly data and the SGI was calculated using a non-parametric distribution for monthly hydraulic head values. The probabilities associated with the fitted distribution were converted into the index values using an inverse normal cumulative distribution function. The SPI was computed using the *SPEI* R package with a gamma distribution, the STI was computed using the *STI* R package with a normal distribution, and the SGI was computed using the code of the SGI function in the *Pastas* Python package based on Bloomfield and Marchant (2013). Following the classification suggested by McKee et al. (1993), the index values were categorized into different drought- and wet-condition intensity levels for the SPI and SGI. Index values were also categorized according to conditions that were colder than, warmer than, or at the normal temperatures for the STI. The categories were therefore: extreme drought or extremely cold (index ≤ -2), severe drought or very cold (-2 < index value ≤ -1.5), moderate drought or moderately cold (-1.5 < index ≤ -1.0), minor drought or slightly cold (-1 < index ≤ -0.5), normal conditions (-0.5 < index ≤ 0.5), and the inverse for wet and warm conditions.

Daily precipitation and temperature data were aggregated for each of

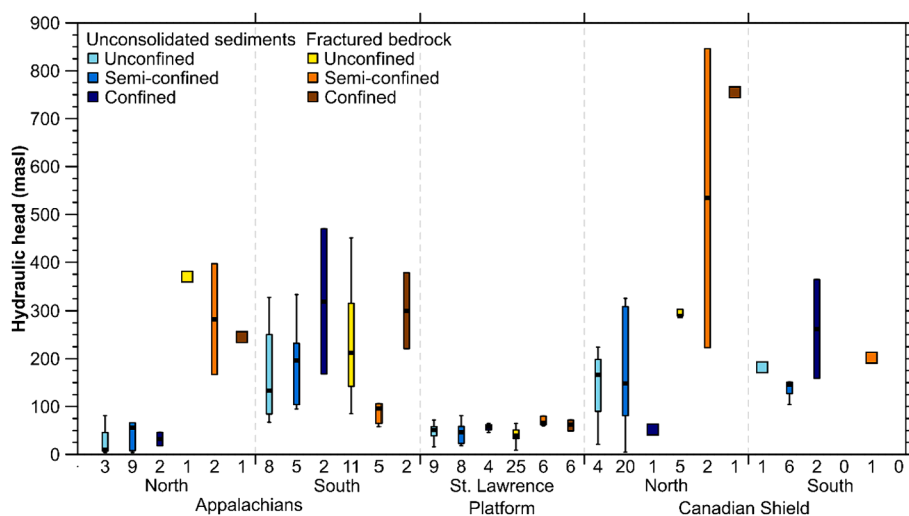


Fig. 3. Average hydraulic heads based on the geological region and the confining conditions. The number of wells in each category is indicated under each box plot (below the x-axis) for a total number of 152 wells. There are more than 10 years of data for each well during the 2000–2022 period.

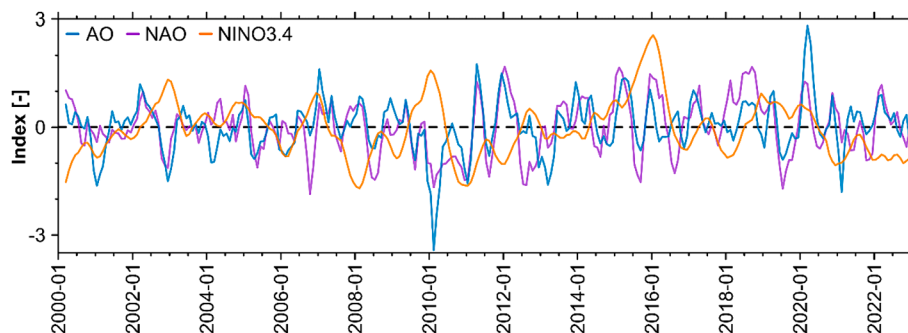


Fig. 4. Three-month rolling average for the Arctic oscillation (AO), North Atlantic oscillation (NAO), and Nino 3.4 (NINO3.4) indexes during the 2000–2022 period.

the five geological regions with a monthly time step to determine the SPI and STI. Daily groundwater level data were averaged to monthly time steps for each observation well to calculate the SGI. The average SGI and its standard deviation were calculated for each of the five geological regions. Autocorrelation of SGI time series was calculated for each observation well and then averaged for each geological region. Aquifer memory is defined as the period of influence that a particular SGI value could have on the months that follow. It is associated with the number of months needed to reach autocorrelation values  $< 0.1$ , a threshold similar to that used by Bloomfield and Marchant (2013). To identify how precipitation and temperature affect groundwater levels, cross-correlations between the SPI and STI as input signals and the SGI as the output signal were calculated for each geological region. For these calculations, averaged regional SPI and STI values (input signals) and SGI values of each well of the geological region (output signal) were used. Cross-correlograms were further averaged for each geological region. Cross-correlations were also performed using the three climate indexes as input signals (AO, NAO, and NINO3.4), with the SPI, STI, and SGI as output signals.

The STI and SGI are continuous variables of monthly temperature and monthly hydraulic heads, respectively and neither require an accumulation period, unlike the SPI for monthly precipitation (Bloomfield and Marchant, 2013; McKee et al., 1993; Zscheischler et al., 2014). It was necessary to determine which accumulation period was most suited for calculating the SPI when used with the SGI to perform cross-correlations. We selected the period that yielded the highest cross-correlation coefficient between the SPI as the input signal and SGI as the output signal, similar to the approach suggested by Bloomfield and Marchant (2013).

## 4. Results

### 4.1. Trends

#### 4.1.1. Regional precipitation and regional temperature

Significant trends in precipitation were positive, except for the Canadian Shield North. The average significant trends varied from  $-0.02$  cm/yr in the Canadian Shield North (77 % of the cells showed statistically significant trends) to  $+0.06$  cm/yr in the Canadian Shield South (61 % of cells showed significant trends) (Fig. 5; Supplementary Fig. A1). While the uncertainty in precipitation trends (estimated with the standard deviation) was generally low for most regions, it was relatively higher in the Canadian Shield North. Significant regional trends in temperature were consistently positive throughout the study area, and with minimal uncertainty. The warming rates ranged from  $+0.05$  °C/yr in the Canadian Shield South (19 % of cells showed significant trends) to  $+0.06$  °C/yr in the Appalachians North (44 % of cells showed significant trends).

#### 4.1.2. Regional hydraulic head

Significant trends in hydraulic heads were negative on average,

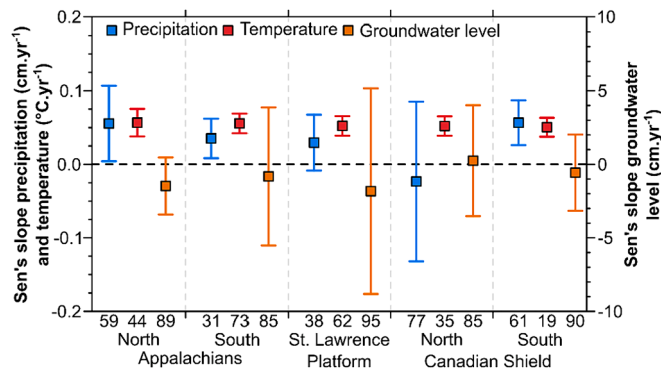


Fig. 5. Significant annual trends in precipitation, temperature, and hydraulic heads for each geological region during the 2000–2022 period (square = mean, whiskers =  $\pm$  standard deviation). The percentages of cells and observation wells with significant trends are indicated under each box plot (below the x-axis). Left y-axis displays the scales of both precipitation trends (in  $\text{cm.yr}^{-1}$ ) and temperature trends ( $^{\circ}\text{C.yr}^{-1}$ ).

indicating a general decrease in groundwater levels. However, an exception was observed for wells located in the Canadian Shield North, which exhibited a slightly positive average trend. The trends in groundwater levels varied from  $-1.8$  cm/yr in the St. Lawrence Platform (95 % of the wells showed significant trends) to  $+0.2$  cm/yr in the Canadian Shield North (85 % of the wells showed significant trends) (Fig. 5). While significant trends were identified in most wells located in the study area, their spatial variability was relatively high, both in terms of trend direction and trend intensity, leading to a high level of uncertainty (Fig. 5; Supplementary Fig. A1).

### 4.2. Standardized signals

#### 4.2.1. Meteorological conditions

SPI values showed that wet and dry periods occurred in rapid succession, with only a few periods of consistent wet or dry state that occurred simultaneously in the five regions (Fig. 6). In 2003, all regions experienced a wet period ( $1.5 < \text{SPI} < 2.5$ ) that lasted less than a year. All regions also experienced a dry period ( $-3 < \text{SPI} < 0$ ) that started at the end of 2009 and lasted for one year, and another dry period ( $-3 < \text{SPI} < 0$ ; except in the Appalachians North) that started in summer 2021 and lasted for one year. This last dry period was most intense in the Appalachians South and in the St. Lawrence Platform, where it started even earlier (early 2020). Atmospheric drought conditions ( $\text{SPI} < -0.5$ ) lasted for limited periods of time, with average durations between 4 months in the Appalachians North and 9 months in the Canadian Shield South. Maximum drought durations were  $> 1$  year in all regions (Fig. 9).

STI values exhibited series of warm and cold periods that were simultaneous and consistent in duration and intensity across the study area (Fig. 6). A warm period with an  $\text{STI} > 1$  started during the second

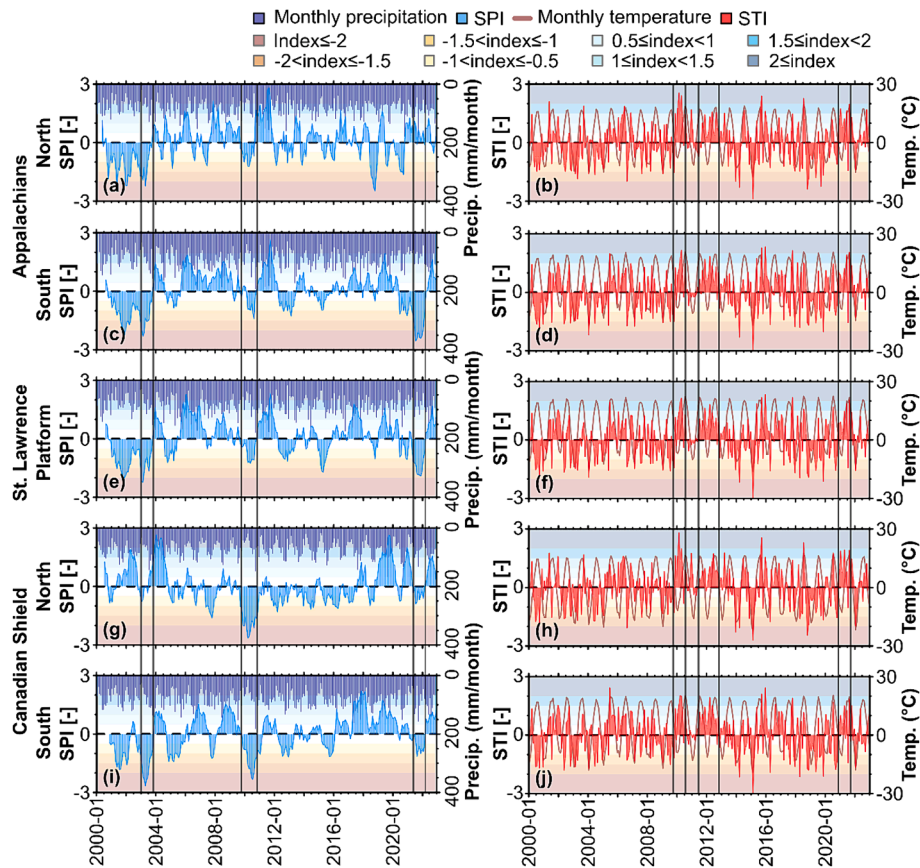


**Fig. 6.** (a, c, e, g, i) Average monthly total precipitation and standardized precipitation index (SPI), and (b, d, f, h, j) average monthly temperature and standardized temperature index (STI) for each geological region. The SPI values were calculated using the optimized accumulation period. Gridded values of precipitation and temperature were averaged over each geological region to compute average SPI and STI values.

half of 2009 and lasted for a year, a second one started in mid-2011 and lasted until the end of 2012, and a third warm period with  $1.5 < STI < 2$  occurred from end of 2020 to end of 2021. Few extremely hot periods were observed in summer 2011. Cold periods ( $STI < 0$ ) appeared to be more random and occurred less consistently than warm periods. They had short durations ( $\sim$ month) with temperatures far below the average values, at  $-3 < STI < -2$  with minimum values reached in the first part of 2015.

#### 4.2.2. Hydraulic heads

SGI values were similarly low in all five geological regions during the same years (Fig. 7a) with a period of a minor drought to moderate drought observed in 2012 ( $SGI < -0.5$  and in some places  $SGI < -1.5$ ). This was followed by more severe episodes of low hydraulic heads during the winter of 2014–2015, which were most noticeable in the St. Lawrence Platform ( $-1.5 < SGI < -1$ ; moderate drought), and during the summer of 2020 in both parts of the Appalachians and the St. Lawrence Platform ( $SGI < -1.5$  and in some places  $SGI < -2$ ; severe to extreme drought). From spring 2021 to summer 2022, wells across the study area except in the Appalachians North also exhibited continued low hydraulic heads associated with SGI values for severe to extreme drought ( $SGI < -1.5$  and in some places  $SGI < -2$ ). When averaged for each geological region, the SGI time series exhibited relatively limited uncertainty, with the largest uncertainty observed in both region of the Canadian shield (Fig. 7b–f).

SGI autocorrelations showed that the aquifer memory was 11 months in the Appalachians (North and South), 19 months in the St. Lawrence Platform, 9 months in the Canadian Shield North and 8 months in the Canadian Shield South (Fig. 8a, c, e, g, i). Drought conditions ( $SGI < -0.5$ ) only lasted for short periods of time, with average durations

between 2.5 months in the Appalachians North and 4 months in the Canadian Shield (both North and South) (Fig. 7; Fig. 9). There were no significant trends in the duration of these droughts. The longest drought that was recorded for every observation well was averaged for each geological region (referred to as the maximum drought duration) and ranged between 8.5 months in the Appalachians North and 15.2 months in the St. Lawrence Platform.

#### 4.3. Cross-correlations between SPI, STI, and SGI

The maximum cross-correlation coefficients between the SPI (input signal) and the SGI (output signal) were obtained with SPI accumulation periods that were  $< 12$  months (Supplementary Fig. A2). The optimal accumulation periods ranged between 5 months in the Appalachians North and 11 months in the Canadian Shield South and were used to conduct the cross-correlation analyses between the SPI (input signal) and the SGI (output signal) for each geological region.

Maximum cross-correlation values between the SPI (with optimized accumulation periods) and the SGI were systematically obtained for a lag of 0 month and ranged between 0.19 in the Canadian Shield North and 0.43 in the Appalachians South (Fig. 8b, d, f, h, j; Fig. 10). Maximum cross-correlation values between the STI and the SGI were equal to 0.09 in the Appalachians South (lag = 57 months), the St. Lawrence Platform (lag = 50 months), and the Canadian Shield North (lag = 43 months) (Fig. 8b, d, f, h, j; Fig. 10). Maximum cross-correlation values between the STI and the SGI were equal to 0.15 in the Appalachians North and the Canadian Shield South (lag = 0 month).

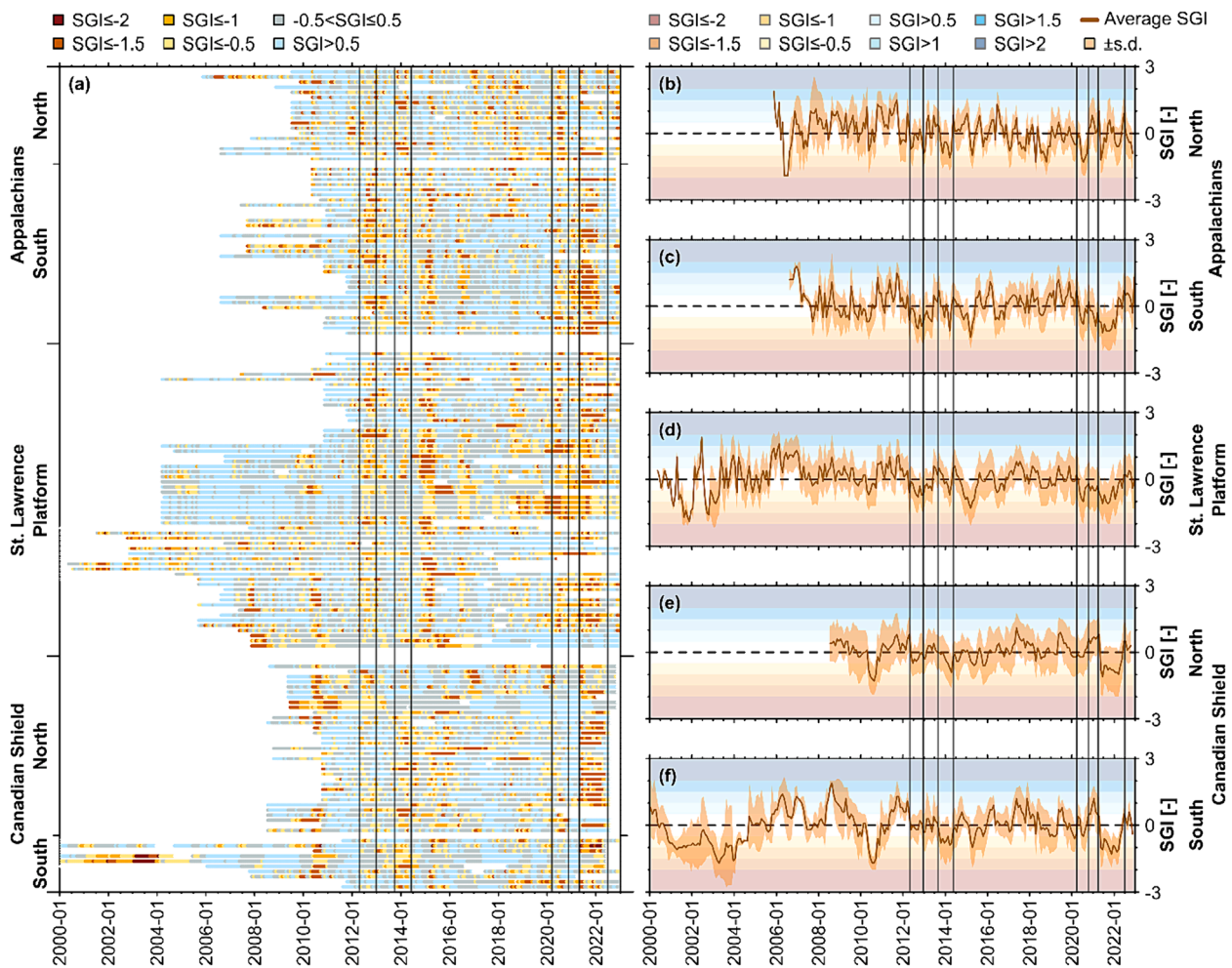


Fig. 7. (a) Standardized groundwater index (SGI; monthly time step) calculated for each observation well with more than 10 years of data and (b to f) average and standard deviation of the SGI values for each geological region.

4.4. Cross-correlations between global climate indexes and SPI, STI, and SGI

The cross-correlation analysis of the three selected global climate indexes (AO, NAO, and NINO3.4) as input signals and the SPI, STI, and SGI as output signals showed that the highest absolute cross-correlation values were systematically obtained with NINO3.4 for the five geological regions (Fig. 10; Supplementary Fig. A3). However, maximum absolute values of cross-correlations between AO and NAO and SGI were similar to those between NINO3.4 and SGI.

5. Discussion

5.1. Changes through time

This study presents the first evidence of a slight decrease in groundwater levels over the past two decades in the province of Quebec (Fig. 5). This trend was visible in the Appalachians, the St. Lawrence Platform, and the Canadian Shield South (maximum decrease of -1.8 cm/yr in the St. Lawrence Platform). The spatial variability of trends in groundwater levels for each region is noteworthy (Supplementary Fig. A1). Although the Appalachians North showed consistently decreasing groundwater levels, the Appalachians South showed a mix of increasing and decreasing levels. The St. Lawrence Platform exhibited the greatest variability in trends. Because these decreasing trends were not consistent with the slight increases in precipitation, it is possible that

they were linked to drivers such as changes in groundwater recharge dynamics and a warming climate that increases the evapotranspiration demand and the need for water supply, for example through irrigation. It is also possible that anthropogenic changes in land use and land cover such as urban sprawl or draining of wetlands contributed to reduce groundwater levels.

The contrasting trends could be related to the presence of confined, semi-confined, and unconfined conditions in the Appalachians South and in the St. Lawrence Platform. In these regions, wells are exposed to variable recharge rates ranging from important seasonal recharge in unconfined conditions to limited and relatively constant recharge rates in confined conditions. Confining conditions are less prevalent in the other regions and groundwater recharge dynamics are likely more homogeneous. Interestingly, Nygren et al. (2021) reported on spatial heterogeneities of similar amplitudes with decreasing groundwater levels in Finland and increasing groundwater levels in southwestern Sweden between 1980 and 2010.

Interestingly, between 1961 and 2017, Dubois et al. (2021) did not observe decreases in groundwater recharge in southern Quebec that were significant enough to explain the decreasing groundwater levels observed in this study. Hodgkins et al. (2017) and Dudley and Hodgkins (2013) observed mainly increasing trends in groundwater levels in the northeast and north-central USA between the 1960s and the early 2010s. It is possible that recharge rates have only recently started to markedly decrease and that the repercussions of this decrease were not perceptible in earlier studies. It is also possible that stable or increasing precipitation

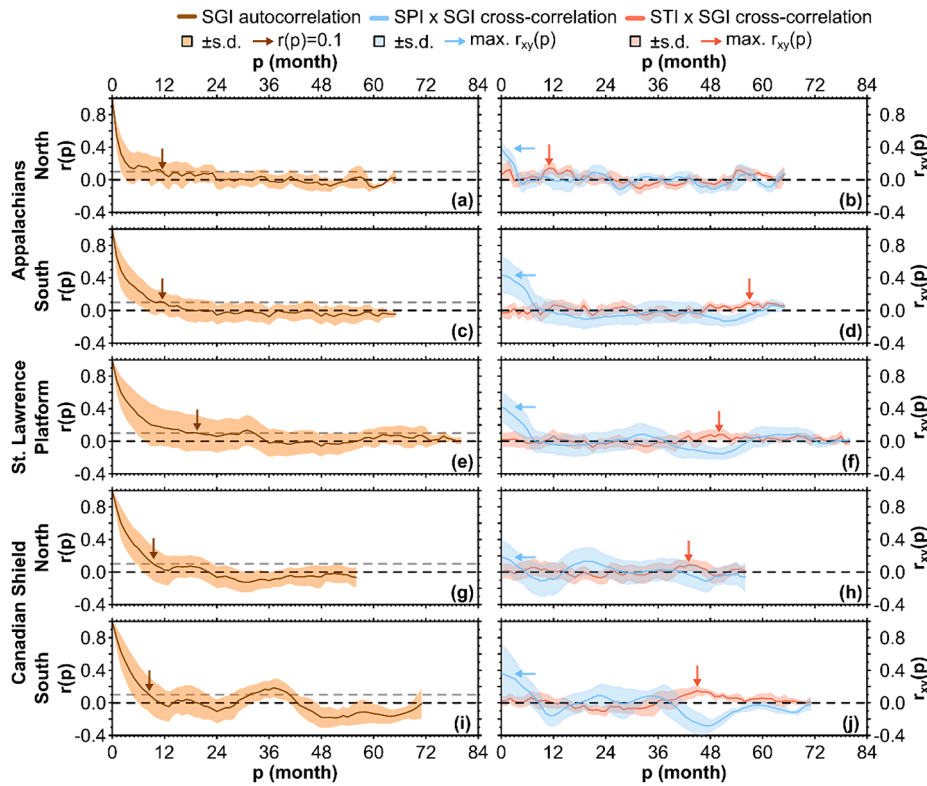


Fig. 8. Average and standard deviation of (a, c, e, g, i) autocorrelations  $r(p)$  for SGI, and (b, d, f, h, j) cross-correlations between the SPI (using optimized accumulation period), STI (input signals), and SGI (output signal) for each geological region. Grey dashed lines represent the 0.1 thresholds.

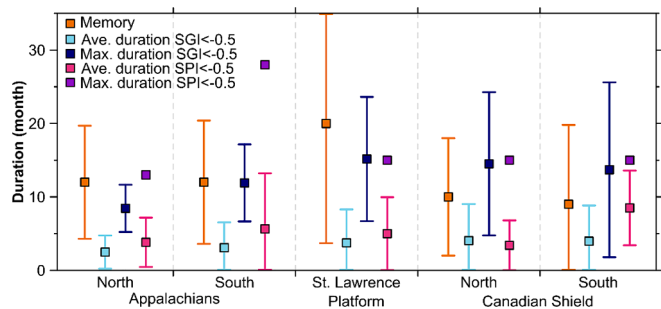


Fig. 9. Aquifer memory (lag duration to attain  $r(p) = 0.1$  for SGI) and average and maximum groundwater and atmospheric drought duration defined as periods  $> 1$  month with  $SGI < -0.5$  and  $SPI < -0.5$  (whiskers =  $\pm$  standard deviation).

are not resulting in higher groundwater levels because evapotranspiration rates might also have markedly increased (Bloomfield et al., 2019). Declining groundwater levels and relatively stable recharge might also be explained by increases in groundwater pumping rates. Drier conditions and warmer temperatures may increase groundwater pumping rates and thus decrease groundwater levels. Although estimated pumping rates are well below the recharge rates at the regional scale in the province of Quebec (see recent groundwater characterization reports in MELCCFP, 2023c), local groundwater extraction rates are not available.

Bloomfield et al. (2019) showed that the frequency, magnitude, and intensity of groundwater droughts increased in the UK, with intense hydrological droughts occurring over large territories for both surface water and groundwater, simultaneously (Marsh et al., 2007). These droughts were not observed in the province of Quebec over the last two decades, but the longer-lasting and widespread low groundwater levels identified in 2020–2021 could be an indication of changing conditions.

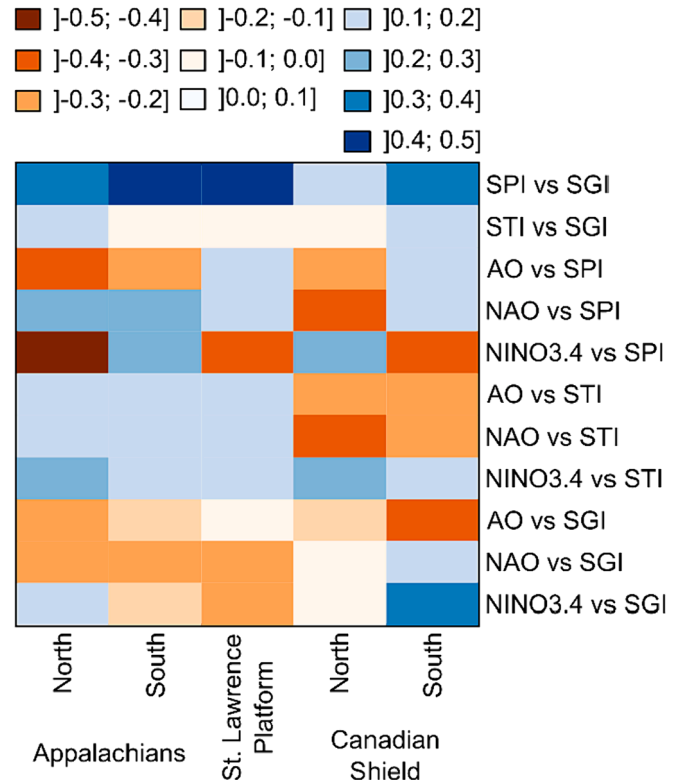


Fig. 10. Maximum cross-correlation between the SPI (optimized accumulation period), STI (input signals), and SGI (output signal), and between AO, NAO, and NINO3.4 (input signals), and the SPI (optimized accumulation period), STI, and SGI (output signals).

The slow rates of decline in groundwater levels observed in Quebec were of the same orders of magnitude as those reported by Nygren et al. (2021). Although these rates were slow compared to the rates of decline observed in warmer climates (Valois et al., 2020), if sustained over a long period of time, these trends could cause the dewatering of pumps in shallow wells. Jasechko and Perrone (2021) reported that many shallow wells worldwide are at risk of running dry if groundwater levels decrease by only a few meters. Lower groundwater levels can also induce a decrease in river flow rates during the dry season (de Graaf et al., 2019), drying streams in headwater basins (Messenger et al., 2021), and drying wetlands (Wossenyeleh et al., 2021).

## 5.2. Contribution of meteorological conditions to groundwater level fluctuations

### 5.2.1. Meteorological conditions

The simultaneous occurrence of low values for the SGI and SPI (limited precipitation) explained the maximum cross-correlation coefficients obtained with a lag of zero months between the standardized signals (Fig. 8; Fig. 10). The following rapid decrease indicated that precipitation impacted groundwater levels in the short term and did not have a lasting effect on the following seasons or years. This observation was consistent with the optimization of the accumulation period for the SPI (<1 year), emphasizing the relevance of intra-annual SPI fluctuations to explain SGI fluctuations. These results contrasted with the observations from 14 wells in unconfined fractured aquifers in the UK, where maximum cross-correlations between the SPI and SGI were often > 0.5 with lags of > 1 year (Bloomfield and Marchant, 2013). Similarly, Kumar et al. (2016) obtained maximum cross-correlations of mostly > 0.6, but with lags ranging from < 1 year to > 1 year, for 2 040 wells in Germany and the Netherlands. The comparatively lower cross-correlation and short lags observed in this study could be related to the marked effect of winter (October/November to April) on hydrologic processes. During winter, most of precipitation occurs as snowfall and is stored until the end of winter, thereby creating an annual spring thaw event that releases a substantial volume of liquid water (Aygün et al., 2020; Dubois et al., 2021, 2022; Nygren et al., 2020). This seasonal event carries an influx of water to aquifers, becoming the main groundwater recharge period (Dubois et al., 2021; Nygren et al., 2021). This cyclic phenomenon has the potential to reset the groundwater systems from previous dryer conditions, thereby directly contributing to reduce the duration of the impacts of previous atmospheric conditions onto groundwater levels. Verification of this hypothesis requires the simulation of snow accumulation during the winter season (when direct precipitation is zero meaning no liquid water) and the simulation of snowmelt in the spring (when available liquid water is the sum of direct precipitation and snowmelt). Combining these simulations would create a time series of the available liquid water, which could then be compared to the SGI.

The notably lower cross-correlations between the STI and SGI were surprising, considering the significant role of temperature on snow accumulation and melt as well as on evapotranspiration (Aygün et al., 2020) and groundwater recharge (Dubois et al., 2021). However, the impacts of snow processes and evapotranspiration on groundwater level fluctuations are indirectly linked to the temperature, thus probably diminishing the correlation between the STI and SGI. Other studies that examined the correlation between the SGI and meteorological conditions (e.g., Bloomfield and Marchant, 2013; Guo et al., 2021; Kumar et al., 2016) mostly focused on precipitation (SPI) as a predictor of groundwater droughts. For this reason, it was not possible to compare STI results from this study with those from other countries or other climatic conditions.

### 5.2.2. Drought propagation

This study is among the few that assessed hydrogeological droughts in cold and humid climates. Periods of hydrogeological drought

associated with SGI values < -0.5 were observed in each of the geological regions, and these generally lasted < 1 year (Fig. 9). During the most intense drought conditions observed during the 2020 and 2021 hydrological years (both in terms of intensity and spatial coverage), drought conditions lasted > 1 year, but were < 2 years, probably limited by the maximum duration of atmospheric droughts (Fig. 7; Fig. 9). Between 2000 and 2022, no multi-year droughts were observed in the study area. These durations contrasted with the multiannual hydrogeological droughts reported by Marchant and Bloomfield (2018) in Great Britain during the 1960–2013 period and were slightly shorter than the 2-year droughts repeatedly observed by Babre et al. (2022) in the Baltic States during the 1989–2018 period. The shorter hydrogeological droughts could be linked to the combination of mostly short-duration atmospheric droughts and the short memory of the aquifers in the study area.

### 5.2.3. Atmospheric conditions

The clear correlation between the SPI and STI, and NINO3.4 (Fig. 10) was consistent with results from other studies in eastern Canada that reported links between variability in temperature and precipitation and AMO, AO, NAO, NPI, and PDO (Assani et al., 2019; Assani and Guerfi, 2017; Qian et al., 2008; Vincent et al., 2015). These connections between global climate indexes and the SPI or STI were less marked with the SGI (except for the Canadian Shield South). Again, this could be due to the short period of influence of precipitation and temperature on groundwater levels. On the east coast of the USA, Kuss and Gurdak (2014) showed correlations between ENSO or NAO and groundwater levels, which partially explained the intra- and inter-annual variability in groundwater levels. Due to the climate there being milder than in the province of Quebec, groundwater levels were probably less impacted by the cold period.

One of the main contributions of this work was to show that the strong seasonality of groundwater levels linked to the cold period caused an annual reset of the hydrological state of the aquifers, drastically limiting aquifer memory and shortening the duration of hydrogeological droughts in the study area. This means that meteorological conditions influenced groundwater levels only for a short period of time. A similar lack of connection between meteorological conditions and groundwater levels might be expected in other regions where the cold period determines the hydrological dynamics. However, considering the current trends in climate warming, this relationship may change in the future. The current warming temperatures are expected to alter the hydrologic dynamics during cold period (Aygün et al., 2020; Dubois et al., 2022), change climate-groundwater dynamics (Nygren et al., 2020), and potentially increase the amount of time that meteorological conditions influence groundwater level fluctuations, up to multiple years. This could ultimately result in an increased sensitivity of groundwater levels to meteorological conditions and cause longer-lasting effects of changes in meteorological conditions through time.

## 5.3. Other factors that explain groundwater level fluctuations

Groundwater storage in catchments is an important parameter influencing the hydrological response to decreased precipitation or increased temperature. This has been linked to the way groundwater flow contributes to surface water flow during meteorological droughts (Arnoux et al., 2021; Haslinger et al., 2014; alpine and temperate climates). Storage and hydraulic conductivity also likely influence the link between meteorological droughts and groundwater levels. This was shown by Bloomfield and Marchant (2013), who linked the shape of SGI autocorrelograms in the UK to storage and hydraulic conductivity with more rapidly decreasing autocorrelations in fractured aquifers than in unconsolidated aquifers. Although similar observations were expected for the current study, the relatively limited number of wells in each region did not allow to make observations at that level of detail. Confining conditions are another possible factor influencing the shape of

SGI autocorrelograms as the St. Lawrence Platform, which had the highest number of wells in semi-confined and confined conditions, also had the longest aquifer memory (Fig. 3; Fig. 9). Verification of this hypothesis requires access to a more important number of wells in various confining conditions.

The relatively strong positive cross-correlation between the SPI and SGI in the study area contrasted with the results from Guo et al. (2021), who obtained both positive cross-correlations (i.e., higher SPI values inducing higher SGI values, and vice-versa) and negative cross-correlations (i.e., higher SPI values inducing lower SGI values, and vice-versa) in four observation wells located in different regions of the USA (Georgia, Massachusetts, Oklahoma, and Washington). These authors associated negative correlations with anthropogenic impacts on groundwater levels linked to pumping and irrigation. Other studies have also shown that groundwater abstraction affected hydrological drought (Van Loon et al., 2013; Van Loon et al., 2022) and that human activity across the globe exacerbated streamflow droughts (Van Loon et al., 2022; De Graaf et al., 2019). Assani et al (2022) have shown that seasonal daily minimum flows decreased as agricultural surface area in watersheds increased. In their study, pumping for irrigation or livestock water supply and land drainage could be responsible for lower groundwater levels and lower river flows. In the current study, groundwater abstraction and agricultural drainage did not affect the groundwater levels enough to be clearly identifiable in the SGI time series. However, these relationships require further investigation and rigorous quantification of groundwater extraction rates and the impact of drainage. This detailed information is not yet available in the province of Quebec.

#### 5.4. Recommendations

Having access to longer time series might have provided more insight into how meteorological conditions influence groundwater level fluctuations and helped identify significant trends in groundwater levels, as underlined by Rivard et al. (2009). Using longer time series also provides an opportunity to investigate how global climate indexes with longer return periods, such as the AMO (60–80 years) and the PDO (20–30 years), impact groundwater levels. Considering the changing global conditions and the expected impacts on groundwater recharge (Dubois et al., 2022, 2023), long-term monitoring will be crucial to assess the changes in groundwater resources. Nevertheless, this study provides useful insight into the use of relatively short time series to identify general groundwater level trends and the duration of groundwater droughts.

This study investigated a large number of wells, but their density across the study area was sparse, providing only 152 time series over 980 000 km<sup>2</sup>. Increasing the spatial coverage and density of groundwater monitoring networks is a straightforward way to achieve a deeper understanding of the processes involved (see for example the global groundwater platform from Condon et al., 2021). Including more observation wells would also help to understand the contrasting geological and geomorphological conditions throughout the province, such as confinement conditions, aquifer thickness, hydraulic conductivity, storage coefficients, and distance from a river.

To provide information that would be even more useful for integrated water management, groundwater level observation networks could be organized to include monitoring of surface water–groundwater interactions. This could be achieved by including observation wells following river reaches or well-transects that are perpendicular to rivers to investigate how aquifer–river exchanges vary in space and time across a watershed. Although not available in the current study, these types of data would provide crucial information given the sensitivity of streamflows to long-term declines in groundwater levels reported worldwide (de Graaf et al., 2019).

Temporal continuity of data and data quality checks are extremely important in groundwater observation networks. Limiting data

interruptions and providing rigorous quality control contributes to longer and more reliable time series that could lead to more useful results. Monitoring land use and water use changes over time would also provide highly useful data to better understand the variability in the range of groundwater level trends and to distinguish between the effect of meteorological conditions and that of human pressures.

## 6. Conclusion

The objective of this research was to quantify how standardized indexes contribute to understanding the groundwater level fluctuations in response to meteorological conditions in cold and humid climates. Over ten years of groundwater level data from 152 wells located in five geological regions in the province of Quebec were used as part of a case study for the 2000–2022 period. Standardized indexes were extremely useful in this analysis, providing a robust basis for the evaluation of groundwater level fluctuations. Ten-year time series appear to be sufficient to assess trends and causal relationships with the meteorological conditions in a cold and humid climate. However, this period is considered too short to characterize long-term drivers such as multi-decadal climatic cycles and the impacts of anthropogenic changes.

Results showed small but significant trends for increasing precipitation in four of the five regions studied. Temperature increased throughout the study area from 2000 to 2022. Groundwater levels generally decreased slightly but showed high variability in all the regions. The results underlined the responsiveness of groundwater levels and the short-term memory of the aquifers in the study area. Groundwater level fluctuations appeared to be induced by relatively recent conditions of precipitation and temperature, and hydrogeological droughts were limited to one year. This was explained by the combination of relatively short atmospheric droughts associated to the strong seasonality of meteorological conditions with a cold winter, followed by a rapid spring snowmelt that contributed to resetting aquifer conditions every year.

Although longer and more numerous groundwater level time series would allow for more complete analyses of cause-and-effect relationships, this study has shown that these data contain crucial information that can be identified relatively easily with standardized indexes. This study hypothesized that the short-term reactivity of groundwater levels to meteorological conditions in cold and humid climates is a consequence of the dramatic impact of winter on hydrological conditions. The next few years will provide further data for testing this hypothesis as freezing conditions, snow accumulation, and snowmelt rapidly change in a warming climate.

#### CRediT authorship contribution statement

**Emmanuel Dubois:** Writing – review & editing, Writing – original draft, Visualization, Software, Methodology, Formal analysis, Data curation, Conceptualization. **Marie Larocque:** Writing – review & editing, Writing – original draft, Validation, Supervision, Project administration, Methodology, Funding acquisition, Conceptualization.

#### Declaration of competing interest

The authors declare that they have no known competing financial interests or personal relationships that could have appeared to influence the work reported in this paper.

#### Data availability

The datasets used in this work are available here: <https://doi.org/10.5683/SP3/26ROMJ>

## Acknowledgements

The authors acknowledge the Quebec Ministry of the Environment (*ministère de l'Environnement, de la Lutte contre les changements climatiques, de la Faune et des Parcs*) for financially supporting this project. Authors are also grateful to the Open access funding provided by EPFL.

## Appendix A. Supplementary data

Supplementary data to this article can be found online at <https://doi.org/10.1016/j.jhydrol.2024.131105>.

## References

- Arnoux, M., Brunner, P., Schaeffli, B., Mott, R., Cochand, F., Hunkeler, D., 2021. Low-flow behavior of alpine catchments with varying quaternary cover under current and future climatic conditions. *J. Hydrol.* 592, 125591 <https://doi.org/10.1016/j.jhydrol.2020.125591>.
- Assani, A.A., Guerfi, N., 2017. Analysis of the joint link between extreme temperatures, precipitation and climate indices in winter in the three hydroclimate regions of southern Quebec. *Atmos.* 8, 75. <https://doi.org/10.3390/atmos8040075>.
- Assani, A.A., Maloney-Dumont, V., Pothier-Champagne, A., Kinnard, C., Quéssy, J.-F., 2019. Comparison of the temporal variability of summer temperature and rainfall as it relates to climate indices in southern Quebec (Canada). *Theor. Appl. Climatol.* 137, 2425–2435. <https://doi.org/10.1007/s00704-018-2750-8>.
- Assani, A., Zeroual, A., Kinnard, C., Roy, A., 2022. Spatial-temporal variability of seasonal daily minimum flows in southern Quebec: synthesis on the impacts of climate, agriculture and wetlands. *Hydrol. Res.* 53, 1494–1509. <https://doi.org/10.2166/nh.2022.070>.
- Aygün, O., Kinnard, C., Campeau, S., 2020. Impacts of climate change on the hydrology of northern midlatitude cold regions. *Progr. Phys. Geogr.: Earth Environ.* 44, 338–375. <https://doi.org/10.1177/0309133319878123>.
- Babre, A., Kalvāns, A., Avotniece, Z., Retiķe, I., Bikšē, J., Popovs, K., Jemeljanova, M., Zelenkevičs, A., Dēliņa, A., 2022. The use of predefined drought indices for the assessment of groundwater drought episodes in the Baltic States over the period 1989–2018. *J. Hydrol.: Reg. Stud.* 40, 101049 <https://doi.org/10.1016/j.ejrh.2022.101049>.
- Beauchamp, M., Assani, A.A., Landry, R., Massicotte, P., 2015. Temporal variability of the magnitude and timing of winter maximum daily flows in southern Quebec (Canada). *J. Hydrol.* 529, 410–417. <https://doi.org/10.1016/j.jhydrol.2015.07.053>.
- Bergeron, O., 2016. Grilles climatiques quotidiennes du programme de surveillance du climat du Québec, version 2 [user guide 2016 – daily climate grids from the Quebec climate monitoring program, version 2]. *Ministère Du Développement Durable, De L'environnement Et De La Lutte Contre Les Changements Climatiques, Direction Du Suivi De L'état De L'environnement*. Québec City (Canada). Guide d'utilisation 2016.
- Bloomfield, J.P., Marchant, B.P., 2013. Analysis of groundwater drought building on the standardised precipitation index approach. *Hydrol. Earth Syst. Sci.* 17, 4769–4787. <https://doi.org/10.5194/hess-17-4769-2013>.
- Bloomfield, J.P., Marchant, B.P., McKenzie, A.A., 2019. Changes in groundwater drought associated with anthropogenic warming. *Hydrol. Earth Syst. Sci.* 23, 1393–1408. <https://doi.org/10.5194/hess-23-1393-2019>.
- Condon, L.E., Kollet, S., Bierkens, M.F.P., Fogg, G.E., Maxwell, R.M., Hill, M.C., Fransen, H.-J.-H., Verhoef, A., Van Loon, A.F., Sulis, M., Abesser, C., 2021. Global groundwater modeling and monitoring: opportunities and challenges. *e2020WR029500* *Water Resour. Res.* 57. <https://doi.org/10.1029/2020WR029500>.
- Cuthbert, M.O., Gleeson, T., Bierkens, M.F.P., Ferguson, G., Taylor, R.G., 2023. Defining renewable groundwater use and its relevance to sustainable groundwater Management. *e2022WR032831* *Water Resour. Res.* 59. <https://doi.org/10.1029/2022WR032831>.
- de Graaf, I.E.M., Gleeson, T., van Beek, L.P.H. (Rens), Sutanudjaja, E.H., Bierkens, M.F.P., 2019. Environmental flow limits to global groundwater pumping. *Nature* 574, 90–94. <https://doi.org/10.1038/s41586-019-1594-4>.
- Dubois, E., Larocque, M., Gagné, S., Meyzonnat, G., 2021. Simulation of long-term spatiotemporal variations in regional-scale groundwater recharge: contributions of a water budget approach in cold and humid climates. *Hydrol. Earth Syst. Sci.* 25, 6567–6589. <https://doi.org/10.5194/hess-25-6567-2021>.
- Dubois, E., Larocque, M., Gagné, S., Braun, M., 2022. Climate change impacts on groundwater Recharge in cold and humid climates: controlling processes and thresholds. *Climate* 10, 6. <https://doi.org/10.3390/cli10010006>.
- Dubois, E., Larocque, M., Brunner, P., 2023. Impact of land cover changes on long-term regional-scale groundwater recharge simulation in cold and humid climates. *Hydrol. Process.* 37, e14810. <https://doi.org/10.1002/hyp.14810>.
- Dudley, R.W., Hodgkins, G.A., 2013. Historical groundwater trends in northern New England and relations with streamflow and climatic Variables. *JAWRA J. Am. Water Resour. Assoc.* 49, 1198–1212. <https://doi.org/10.1111/jawr.12080>.
- Giese, M., Haaf, E., Heudorfer, B., Barthel, R., 2020. Comparative hydrogeology – reference analysis of groundwater dynamics from neighbouring observation wells. *Hydrol. Sci. J.* 65, 1685–1706. <https://doi.org/10.1080/02626667.2020.1762888>.
- Guo, M., Yue, W., Wang, T., Zheng, N., Wu, L., 2021. Assessing the use of standardized groundwater index for quantifying groundwater drought over the conterminous US. *J. Hydrol.* 598, 126227 <https://doi.org/10.1016/j.jhydrol.2021.126227>.
- Haslinger, K., Koffler, D., Schöner, W., Laaha, G., 2014. Exploring the link between meteorological drought and streamflow: effects of climate-catchment interaction. *Water Resour. Res.* 50, 2468–2487. <https://doi.org/10.1002/2013WR015051>.
- Hellwig, J., de Graaf, I.E.M., Weiler, M., Stahl, K., 2020. Large-scale assessment of delayed groundwater responses to drought. *e2019WR025441* *Water Resour. Res.* 56. <https://doi.org/10.1029/2019WR025441>.
- Hodgkins, G.A., Dudley, R.W., Nielsen, M.G., Renard, B., Qi, S.L., 2017. Groundwater-level trends in the U.S. glacial aquifer system, 1964–2013. *J. Hydrol.* 553, 289–303. <https://doi.org/10.1016/j.jhydrol.2017.07.055>.
- Jackson, C.R., Bloomfield, J.P., Mackay, J.D., 2015. Evidence for changes in historic and future groundwater levels in the UK. *Progr. Phys. Geogr.: Earth Environ.* 39, 49–67. <https://doi.org/10.1177/0309133314550668>.
- Jasechko, S., Perrone, D., 2021. Global groundwater wells at risk of running dry. *Science* 372, 418–421. <https://doi.org/10.1126/science.abc2755>.
- Konapala, G., Mishra, A.K., Wada, Y., Mann, M.E., 2020. Climate change will affect global water availability through compounding changes in seasonal precipitation and evaporation. *Nat. Commun.* 11, 3044. <https://doi.org/10.1038/s41467-020-16757-w>.
- Krogulec, E., 2018. Evaluating the risk of groundwater drought in groundwater-dependent ecosystems in the central part of the Vistula River valley, Poland. *Ecohydrol. Hydrobiol.* 18, 82–91. <https://doi.org/10.1016/j.ecohyd.2017.11.003>.
- Kumar, R., Musuza, J.L., Van Loon, A.F., Teuling, A.J., Barthel, R., Ten Broek, J., Mai, J., Samaniego, L., Attinger, S., 2016. Multiscale evaluation of the Standardized precipitation index as a groundwater drought indicator. *Hydrol. Earth Syst. Sci.* 20, 1117–1131. <https://doi.org/10.5194/hess-20-1117-2016>.
- Kuss, A.J.M., Gurdak, J.J., 2014. Groundwater level response in U.S. principal aquifers to ENSO, NAO, PDO, and AMO. *J. Hydrol.* 519, 1939–1952. <https://doi.org/10.1016/j.jhydrol.2014.09.069>.
- Marchant, B.P., Bloomfield, J.P., 2018. Spatio-temporal modelling of the status of groundwater droughts. *J. Hydrol.* 564, 397–413. <https://doi.org/10.1016/j.jhydrol.2018.07.009>.
- Marsh, T., Cole, G., Wilby, R., 2007. Major droughts in England and Wales, 1800–2006. *Weather* 62, 87–93. <https://doi.org/10.1002/wea.67>.
- Mazouz, R., Assani, A.A., Rodríguez, M.A., 2013. Application of redundancy analysis to hydroclimatology: a case study of spring heavy floods in southern Québec (Canada). *J. Hydrol.* 496, 187–194. <https://doi.org/10.1016/j.jhydrol.2013.05.035>.
- McKee, T.B., Doesken, N.J., Kleist, J., 1993. The relationship of drought frequency and duration time scales. Presented at the 8th Conference on Applied Climatology, Anaheim, California, pp. 179–184.
- MELCCFP, 2022. Bulletin sur l'état des nappes - Printemps 2022 – Sud du fleuve Saint-Laurent [Water table state - Spring 2022 - Southern part of St. Lawrence River]. <https://www.environnement.gouv.qc.ca/eau/piezo/bulletin-2022-printemps.pdf>.
- MELCCFP (Ministère de l'environnement de la Lutte contre les changements climatiques, de la Faune et des Parcs), 2023a. Québec Groundwater Monitoring Network [website]. URL <https://www.environnement.gouv.qc.ca/eau/piezo/index.htm> (accessed 6.6.23).
- MELCCFP, 2023b. Climat survey of Quebec [website]. URL <https://www.environnement.gouv.qc.ca/climat/surveillance/index.asp> (accessed 6.4.23).
- MELCCFP, 2023c. Québec Groundwater Knowledge Acquisition Projects [website]. URL <https://www.environnement.gouv.qc.ca/eau/souterraines/programmes/acquisition-connaissance.htm> (accessed 7.19.23).
- Messenger, M.L., Lehner, B., Cockburn, C., Lamouroux, N., Pella, H., Snelder, T., Tockner, K., Trautmann, T., Watt, C., Detry, T., 2021. Global prevalence of non-perennial rivers and streams. *Nature* 594, 391–397. <https://doi.org/10.1038/s41586-021-03565-5>.
- NOAA, 2023a. Climate Prediction Center [website]. URL [https://www.cpc.ncep.noaa.gov/products/precip/CWlink/daily\\_ao\\_index/teleconnections.shtml](https://www.cpc.ncep.noaa.gov/products/precip/CWlink/daily_ao_index/teleconnections.shtml) (accessed 5.26.23).
- NOAA, 2023b. Niño 3.4 SST Index [website]. Working group on surface pressure. URL <https://psl.noaa.gov/gcos/wgsp/Timeseries/Nino34/> (accessed 5.26.23).
- Nygren, M., Giese, M., Kløve, B., Haaf, E., Rossi, P.M., Barthel, R., 2020. Changes in seasonality of groundwater level fluctuations in a temperate-cold climate transition zone. *Journal of Hydrology X* 8, 100062. <https://doi.org/10.1016/j.hydroa.2020.100062>.
- Nygren, M., Giese, M., Barthel, R., 2021. Recent trends in hydroclimate and groundwater levels in a region with seasonal frost cover. *J. Hydrol.* 602, 126732 <https://doi.org/10.1016/j.jhydrol.2021.126732>.
- Peters, E., Bier, G., van Lanen, H.A.J., Torfs, P.J.J.F., 2006. Propagation and spatial distribution of drought in a groundwater catchment. *J. Hydrol.* 321, 257–275. <https://doi.org/10.1016/j.jhydrol.2005.08.004>.
- Qian, M., Jones, C., Laprise, R., Caya, D., 2008. The influences of NAO and the Hudson Bay sea-ice on the climate of eastern Canada. *Clim. Dyn.* 31, 169–182. <https://doi.org/10.1007/s00382-007-0343-9>.
- Rivard, C., Vigneault, H., Piggott, A.R., Larocque, M., Ancill, F., 2009. Groundwater recharge trends in Canada. *Can. J. Earth Sci.* 46, 841–854. <https://doi.org/10.1139/E09-056>.
- Rivera, A., 2014. Canada's groundwater resources. *Fitzhenry & Whiteside, Markham, ON*.
- Scanlon, B.R., Fakhreddine, S., Rateb, A., de Graaf, I., Famiglietti, J., Gleeson, T., Grafton, R.Q., Jobbagy, E., Kebede, S., Kolusu, S.R., Konikow, L.F., Long, D., Mekonnen, M., Schmied, H.M., Mukherjee, A., MacDonald, A., Reedy, R.C., Shamsudduha, M., Simmons, C.T., Sun, A., Taylor, R.G., Villholth, K.G., Vörösmarty, C.J., Zheng, C., 2023. Global water resources and the role of groundwater in a resilient water future. *Nat. Rev. Earth Environ.* 4, 87–101. <https://doi.org/10.1038/s43017-022-00378-6>.

- Secci, D., Tanda, M.G., D'Oria, M., Todaro, V., Fagandini, C., 2021. Impacts of climate change on groundwater droughts by means of standardized indices and regional climate models. *J. Hydrol.* 603, 127154 <https://doi.org/10.1016/j.jhydrol.2021.127154>.
- SIGEOM, 2023. SIGEOM, Geo-mining interactive map [website]. URL [https://sigeom.mines.gouv.qc.ca/signet/classes/I1108\\_afchCartelIntr](https://sigeom.mines.gouv.qc.ca/signet/classes/I1108_afchCartelIntr) (accessed 4.7.23).
- Tremblay, L., Larocque, M., Anctil, F., Rivard, C., 2011. Teleconnections and interannual variability in Canadian groundwater levels. *J. Hydrol.* 410, 178–188. <https://doi.org/10.1016/j.jhydrol.2011.09.013>.
- Valois, R., MacDonell, S., Núñez Cobo, J.H., Maureira-Cortés, H., 2020. Groundwater level trends and recharge event characterization using historical observed data in semi-arid Chile. *Hydrol. Sci. J.* 65, 597–609. <https://doi.org/10.1080/02626667.2020.1711912>.
- Van Loon, A.F., 2015. Hydrological drought explained. *WIREs. Water* 2, 359–392. <https://doi.org/10.1002/wat2.1085>.
- Van Loon, A.F., Rangelcroft, S., Coxon, G., Werner, M., Wanders, N., Baldassarre, G.D., Tjeldeman, E., Bosman, M., Gleeson, T., Nauditt, A., Aghakouchak, A., Breña-Naranjo, J.A., Cenobio-Cruz, O., Costa, A.C., Fendekova, M., Jewitt, G., Kingston, D. G., Loft, J., Mager, S.M., Mallakpour, I., Masih, I., Maureira-Cortés, H., Toth, E., Oel, P.V., Ogtrop, F.V., Verbist, K., Vidal, J.-P., Wen, L., Yu, M., Yuan, X., Zhang, M., Lanen, H.A.J.V., 2022. Streamflow droughts aggravated by human activities despite management. *Environ. Res. Lett.* 17, 044059 <https://doi.org/10.1088/1748-9326/ac5def>.
- Van Loon, A.F., Van Lanen, H.a.J., 2013. Making the distinction between water scarcity and drought using an observation-modeling framework. *Water Resour. Res.* 49, 1483–1502. <https://doi.org/10.1002/wrcr.20147>.
- Vincent, L.A., Zhang, X., Brown, R.D., Feng, Y., Mekis, E., Milewska, E.J., Wan, H., Wang, X.L., 2015. Observed trends in Canada's climate and influence of low-frequency Variability modes. *J. Clim.* 28, 4545–4560. <https://doi.org/10.1175/JCLI-D-14-00697.1>.
- Wossenyeleh, B.K., Worku, K.A., Verbeiren, B., Huysmans, M., 2021. Drought propagation and its impact on groundwater hydrology of wetlands: a case study on the doode bemde nature reserve (Belgium). *Nat. Hazards Earth Syst. Sci.* 21, 39–51. <https://doi.org/10.5194/nhess-21-39-2021>.
- Zscheischler, J., Michalak, A.M., Schwalm, C., Mahecha, M.D., Huntzinger, D.N., Reichstein, M., Berthier, G., Ciais, P., Cook, R.B., El-Masri, B., Huang, M., Ito, A., Jain, A., King, A., Lei, H., Lu, C., Mao, J., Peng, S., Poulter, B., Ricciuto, D., Shi, X., Tao, B., Tian, H., Viogy, N., Wang, W., Wei, Y., Yang, J., Zeng, N., 2014. Impact of large-scale climate extremes on biospheric carbon fluxes: an intercomparison based on MsTMIP data. *Global Biogeochem. Cycles* 28, 585–600. <https://doi.org/10.1002/2014GB004826>.